Journal of The Electrochemical Society, **152** (5) E176-E183 (2005)
0013-4651/2005/152(5)/E176/8/$7.00 © The Electrochemical Society, Inc.

Importance of Oxides in Carbon/Molecule/Metal Molecular Junctions with Titanium and Copper Top Contacts

William R. McGovern,* Franklin Anariba, and Richard L. McCreery,z**

Department of Chemistry, The Ohio State University, Columbus, Ohio 43210, USA

Carbon/molecule/metal molecular junctions were fabricated by metal deposition of titanium or copper on monolayers of nitroazobenzene (NAB), biphenyl, and nitrobiphenyl (NBP), and multilayers of NAB and NBP covalently bonded to an sp^2 carbon substrate. The electronic behavior of Ti junctions was extremely dependent on residual gas pressure during E-beam deposition, due to the formation of a disordered Ti oxyhydroxide deposit. The junction resistance decreased with decreasing residual gas pressure, and the hysteresis and rectification observed previously for relatively high deposition pressure was absent for pressures below 5×10^{-7} Torr. Deletion of the molecular layer resulted in low-resistance junctions for both high and low deposition pressures. Replacement of the Ti with Al with otherwise identical deposition conditions resulted in insulating junctions with much higher resistance and no rectification. Ti junctions made at low residual gas pressure had resistances and current/voltage characteristics similar to those of junctions with Cu top contacts, with the latter exhibiting high yield and good reproducibility. The current/voltage characteristics of both the Ti and Cu junctions fabricated with low residual gas pressure were nonlinear and showed a strong dependence on the molecular layer thickness. The hysteresis and rectification previously observed for junctions fabricated at relatively high residual gas pressure depend on the combination of the NAB layer and the semiconducting TiO_x film, with the TiO_x layer conductivity depending strongly on formation conditions. Rectification and hysteresis in NAB/TiO_x junctions may result from either redox reactions of the NAB and TiO_x layers, or from electron injection into the conduction band of Ti oxide.
© 2005 The Electrochemical Society. [DOI: 10.1149/1.1888369] All rights reserved.

Manuscript submitted July 22, 2004; revised manuscript received November 5, 2004. Available electronically April 7, 2005.

A significant problem with investigation of metal/molecule/metal molecular electronic junctions has been fabrication of the top metal "contact." Vapor deposition of Au or Ag often results in metal penetration into a molecular monolayer, unless there is a reaction between the vapor metal atoms and the monolayer end group.[1-5] Vapor-deposited titanium metal has been investigated as a top contact for various molecular electronic junctions, including metal/molecule/metal junctions based on self-assembled monolayer (SAM)[6,7] and Langmuir-Blodgett (LB) structures.[8-10] Ti atoms are strongly reducing and reactive, and they have been shown to destroy Au/thiol self-assembled aliphatic monolayers, as judged by loss of Secondary-ion mass spectrometry signals from the monolayer.[11] Fourier transform of SAM and LB structures following Ti deposition showed total signal loss for aliphatic or phenylethynyl monolayers,[12] although a naphthalene center was apparently unaffected.[7] We reported recently on carbon/nitroazobenzene (NAB)/Ti molecular junctions which have covalent bonds between the molecule and both the carbon substrate and Ti top contacts.[13] These junctions showed strong rectification, with the current under positive bias (carbon positive of Ti) exceeding that for negative bias by a factor of ~600 at 3 V. Raman spectroscopy and X-ray photoelectron spectroscopy (XPS) demonstrated that a nitroterminated molecular layer was not significantly affected by E-beam deposition of Ti, except for formation of a Ti-N bond and partial reduction of the nitro group.[13,14] Because covalent bonding between the molecular layer and the contacts is often desirable to reduce barriers to electron transport, the top contact metal should be reactive enough to form such bonds, but not so aggressive that it destroys the monolayer or creates metallic short circuits.

Subsequent to our initial report on carbon/NAB/Ti junctions, we observed that junction properties were dependent on Ti deposition rate and the base pressure of the E-beam evaporation chamber.[15] Specifically, a decrease in residual gas pressure from 8×10^{-6} to 5×10^{-7} Torr or less caused a dramatic decrease in junction resistance and apparent loss of hysteresis. SAM and LB junctions reported by others to date were made with residual gas pressures ranging from $<1 \times 10^{-8}$ to $<1 \times 10^{-6}$ Torr,[5-9] and may be subject to the same variation in properties due to trace gases. The current report discusses the effects of Ti oxide formation on junction behavior and reports a means to avoid such effects using copper as the top metal.

Experimental

Molecular junctions with a 3.7 nm thick NAB film were fabricated on pyrolyzed photoresist films (PPFs, rms roughness <0.5 nm) using the procedure described in detail previously,[13] with the important exception of the Ti deposition procedure. PPF is disordered, sp^2 hybridized carbon, with no observable bandgap and essentially metallic conductivity (resistivity ~0.005 Ω-cm).[16,17] For the samples designated as "low oxide," the E-beam evaporation chamber pressure was decreased to several residual gas pressures below 5×10^{-7} Torr, instead of the previous 8×10^{-6} Torr, and the initial Ti deposition rate was increased to 0.1 nm/s compared to the previous 0.03 nm/s. Based on the simple formula that the time required in seconds for a monolayer of collisions between a trace gas and a surface is approximately $(2.5 \times 10^{-6})/P$ (Torr)[18] and that every collision of Ti with water or O_2 is reactive, we predict a substantial fraction of the deposited Ti layer to be Ti oxide or hydroxide. We refer to films deposited using the previous conditions[13] as "high oxide" and those with a pressure of $<5 \times 10^{-7}$ Torr as "low oxide." Note that high oxide and low oxide PPF/NAB(3.7)/Ti/Au junctions are identical except for Ti deposition conditions, with identical PPF substrate, 3.7 nm thick NAB layer, and protective gold layer. In addition, several samples were prepared with aluminum substituted for Ti to investigate the effect of an insulating rather than semiconducting oxide. Deposition conditions for Al were identical to the Ti high oxide case, including the protective Au top layer. Biphenyl (BP) and nitrobiphenyl (NBP) junctions were prepared in the same fashion, using conditions that yield known layer thicknesses as determined with atomic force microscopy (AFM).[19] Junctions are designated as, *e.g.*, PPF/NAB(3.7)/Ti/Au, PPF/NBP(4.2)/Ti/Au, where the thickness of the molecular layer determined with AFM is given in parentheses with units of nanometers. All junctions were 0.5 mm diam (area 0.00196 cm^2, corresponding to ~10^{11} molecules arranged in parallel) with 8-14 junctions per sample. In summary, four metal deposition programs were used: "high oxide Ti": 8×10^{-6} Torr, 3 nm Ti at 0.03 nm/s, 5 min wait, 10 nm Ti at 0.1 nm/s, 40 nm Ti at 1 nm/s, 100 nm Au at 1 nm/s; "low oxide Ti": $(2.1\text{-}5.0) \times 10^{-7}$ Torr (as specified below), 10 nm Ti at 0.1 nm/s, 40 nm Ti at 1 nm/s, 100 nm Au at 1.0 nm/s; "Cu": pressure as specified, 10 nm Cu at 0.1 nm/s, 20 nm Cu at 0.5 nm/s, 10 nm Au at 1.0 nm/s; and "high oxide Al": 3 nm Al at 0.03 nm/s, 5 min wait, 10 nm Al at

* Electrochemical Society Student Member.
** Electrochemical Society Fellow.
z E-mail: mccreery.2@osu.edu

Table I. PPF/molecule/Ti/Au junction results.

Molecule[a]	Samples	Junctions	Resistance[b] (Ω)	J (+2 V) (A/cm^2)	J (−2 V) (A/cm^2)	dV/di (+2 V)
BP (1.5)[c]	1	13/14	6460 ± 3200 (50%)	2.70 ± 0.45 (17%)	2.61 ± 0.47 (18%)	188 ± 10 (5.1%)
NBP (1.7)	2	28/28	188 ± 55 (29%)	4.75 ± 0.51 (11%)	4.68 ± 0.54 (11%)	168 ± 30 (18%)
NBP (4.2)	2	25/28	17,200 ± 6000 (35%)	2.33 ± 0.57 (24%)	1.75 ± 0.36 (21%)	238 ± 48 (20%)
NBP (4.8)	2	28/28	39,300 ± 9200 (23%)	2.01 ± 0.25 (12%)	1.47 ± 0.19 (13%)	250 ± 22 (8.7%)
NAB (1.8)	2	8/8	840 ± 610 (73%)	>5[e]	>5[e]	-[e]
NAB (3.7)[d]	2	8/8	3100 ± 1500 (48%)	3.29 ± 1.04 (31%)	2.96 ± 1.09 (37%)	204 ± 46 (22%)
NAB (4.2)[d]	1	4/4	30,800 ± 28,000 (92%)	2.04 ± 0.06 (2.9%)	1.63 ± 0.021 (1.3%)	237 ± 5.3 (2.2%)
Molecule absent	1	7/7	236 ± 14 (5.9%)			

[a] Pressure during Ti deposition was 2.7 × 10^{-7} Torr unless indicated otherwise.
[b] Inverse slope of i/V curve (dV/di) for V = ±50 mV. Listed as mean ± standard deviation, with % relative standard deviation in parentheses.
[c] Number in parentheses is thickness of molecular layer in nanometers.
[d] Ti deposited at 2.1 × 10^{-7} Torr.
[e] Exceeded instrumental limit.

0.1 nm/s, 40 nm Al at 1 nm/s, 100 nm Au at 1 nm/s. Contact was made to the junction as described previously with a Pt wire and a micromanipulator.[13] A few junctions were rejected due to nonrepeatable i/V curves, and standard deviations of the remaining junctions are reported in Tables I and II. As noted in the main text, the Ti junctions slowly became less conductive upon exposure to air, so all electronic measurements reported occurred one day after metal deposition. The junction resistance for low bias was determined as the inverse of the slope of the i/V curve over the range −50 mV $< V <$ +50 mV, and dV/di (+2 V) is the inverse slope of the i/V curve for V = 1.95 to 2.00 V. Positive V corresponds to the PPF contact being more positive than the Ti/Au contact in all cases. XPS spectra were obtained with a Kratos Axis Ultra spectrometer. Except as noted, the sample was transferred through ambient air to the XPS sample introduction chamber immediately after metal deposition. Control junctions were prepared identically to those described previously, but without deposition of the molecular layer, for all three top contacts: Cu, low oxide Ti, and high oxide Ti.

Results

The effect of residual gas pressure on the current/voltage (i/V) response of PPF/NAB(3.7)/Ti/Au junctions is shown in Fig. 1, with the ordinate expressed as current density (J, in A/cm^2). The curve for 8 × 10^{-6} Torr is similar to that reported in detail previously,[13] showing hysteresis for positive voltage and a large resistance at low voltage (685 MΩ). For lower pressures, the resistance at low voltage decreases to 127 ± 21 kΩ for 4.0 × 10^{-7} Torr, 17.5 ± 6.6 kΩ for 2.8 × 10^{-7} Torr, and 3.1 ± 1.5 kΩ for 2.1 × 10^{-7} Torr. Compared to the high oxide junctions, the low oxide junctions exhibited much higher current, little or no hysteresis, and negligible dependence on scan rate. The i/V curves were repeatable in the ±2 V range for thousands of cycles, with no apparent degradation. To determine if the effect of residual gas pressure was observed for a molecule other than NAB, junctions were prepared with BP substituted for NAB. As shown in Fig. 2, the PPF/BP(1.5)/Ti/Au junctions had qualitatively similar i/V responses, with larger currents for the low oxide junctions. The currents observed for the high oxide case were smaller than those for NAB(3.7), and hysteresis was observed for both positive and negative voltage scans. Also shown in Fig. 1 are control junctions with no molecular layer, which have linear i/V responses with slopes corresponding to resistances of 238 Ω (8.0 × 10^{-6} Torr) and 247 Ω (2.1 × 10^{-7} Torr).

The presence of Ti oxide was confirmed with XPS depth profiling of a PPF/azobenzene/Ti/Au molecular junction. Azobenzene was used instead of NAB so the molecule did not contribute oxygen, but the metal deposition conditions were identical to those for NAB and BP. After insertion of the completed sample into the XPS chamber, the metal layers were sputtered with Ar^+ ions and XPS spectra were acquired periodically. Various Ti oxides were observed near the azobenzene layer, including TiO (Ti $2p_{3/2}$ peak at 454.8 eV),[20,21] Ti_2O_3 (456.1 eV),[21,22] and a small amount of TiO_2 (458.8 eV).[21,23] Figure 3 shows high-resolution XPS spectra of the Ti_{2p} region obtained near the azobenzene layer for high oxide (8 × 10^{-6} Torr) and low oxide (2.1 × 10^{-7} Torr) PPF/AB/Ti/Au junctions. Although there are variations in the distribution of Ti and Ti oxides for the two

Table II. PPF/molecule/Cu/Au junction results.

Molecule[a]	Samples	Junctions	Resistance[b] (Ω)	J (+2 V) (A/cm^2)	J (−2 V) (A/cm^2)	dV/dI (+2)
BP (1.5)[c]	2	21/21	315 ± 82 (26%)	4.72 ± 0.51 (11%)	4.54 ± 0.60 (13%)	176 ± 13 (7.2%)
NBP (1.7)	2	28/28	267 ± 59 (22%)	3.85 ± 0.42 (11%)	3.74 ± 0.44 (12%)	191 ± 15 (7.7%)
NBP (2.5)	2	28/28	690.2 ± 71.6 (10.4%)	3.45 ± 0.21 (6.0%)	3.22 ± 0.20 (6.2%)	186 ± 5 (2.9%)
NBP (4.2)	2	28/28	2072 ± 424 (21%)	2.60 ± 0.85 (33%)	2.60 ± 0.85 (33%)	252 ± 79 (31%)
NBP(4.8)	2	28/28	5070 ± 790 (15.7%)	1.98 ± 0.58 (29%)	1.73 ± 0.54 (31%)	301 ± 92 (30%)
NAB (1.8)[e]	2	8/8	443 ± 208 (49%)	4.38 ± 0.64 (13%)	4.34 ± 0.66 (15%)	192 ± 21 (11%)
NAB (3.7)[e]	2	8/8	1490 ± 810 (54%)	4.18 ± 0.99 (24%)	4.05 ± 1.12 (28%)	175 ± 37 (21%)
NAB (4.2)[e]	2	8/8	8040 ± 1950 (28%)	4.04 ± 1.09 (27%)	3.66 ± 1.01 (28%)	177 ± 40 (22%)
Molecule absent	2	18/18	81 ± 6[d]	>5	>5	-

[a] Pressure during Cu deposition was 2.7 × 10^{-7} Torr unless indicated otherwise.
[b] Inverse slope of i/V curve (dV/di) for V = ±50 mV.
[c] Number in parentheses is thickness of molecular layer in nanometers.
[d] Cu deposited at 2.7 × 10^{-7} Torr.
[e] Pressure during Cu deposition was 4.5 × 10^{-7} Torr.

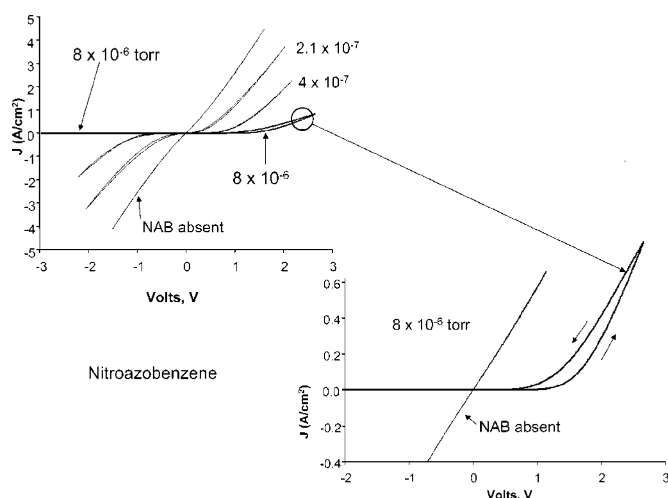

Figure 1. i/V curves for PPF/NAB(3.7)/Ti junctions with Ti deposited at varying residual gas pressures (indicated for each curve in torr). Scan rate was 1 V/s in all cases, and deposition pressure in torr is indicated for each curve. Inset shows high oxide (8×10^{-6} Torr) case with expanded current density scale. Also shown are the linear responses obtained when the molecular layer is absent for PPF/Ti/Au junctions formed at 2.1×10^{-7} (upper panel) and 8×10^{-6} Torr (lower panel).

pressures, clearly even the low oxide case contains significant TiO and Ti_2O_3. The small peak for TiO_2 apparent in the high oxide sample increased with time after deposition, with TiO_2 being the dominant species after 1 year in ambient air (Fig. 3c). High-resolution XPS spectra of the O_{1s} region showed two peaks at 530.5 and 532 eV, which are characteristic of metal oxide (530.5 eV)[23-25] and metal hydroxide (531.7 eV).[23,26-30] The oxyhydroxide deposit is likely to be very disordered and is referred to as TiO_x. Clearly, the 2×10^{-7} Torr base pressure of the E-beam system employed was not sufficiently low to yield a Ti deposit that is uncontaminated by oxides, and also that the TiO_x layer is a structurally complex mixture of Ti in the +2, +3, and +4 oxidation states.

A more detailed examination of the effect of residual gas pressure on the low-bias resistance was conducted for the PPF/NAB(3.7)/Ti/Au case, with the results shown in Fig. 4. The resistance at low voltage decreased monotonically with decreasing pressure, down to the lowest pressure achievable with the apparatus employed, 2.1×10^{-7} Torr. Although a log-log plot of resistance *vs.*

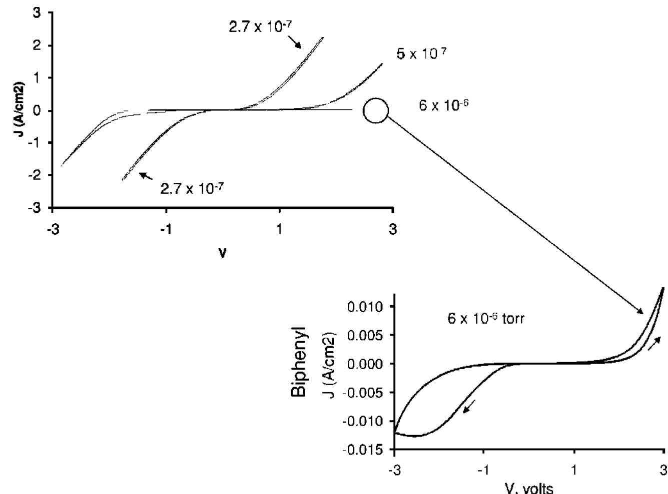

Figure 2. Same as Fig. 1, but for PPF/BP(1.5)/Ti junctions, also at 1 V/s.

pressure was approximately linear, its slope was ~3, indicating a strong, nonlinear dependence on pressure.

As noted, the lowest backpressure employed (2.1×10^{-7} Torr) yielded a Ti deposit that contained significant oxide, making it difficult to evaluate junctions containing only metallic Ti. To circumvent this problem, copper was substituted for Ti to reduce the tendency of the top contact metal to oxidize. J/V curves for low oxide PPF/NAB(3.7)/Ti/Au and PPF/BP(1.5)/Cu/Au junctions are compared in Fig. 5. The Cu junctions had somewhat lower resistance than the Ti junctions at low bias, although the curve shapes were similar. Table II includes resistance values obtained for many Cu junctions, including standard deviations for multiple junctions on two separate samples. The reproducibility of the Cu junctions was significantly better than that of the Ti junctions, and few Cu junctions displayed anomalous behavior. Of the 157 Cu junctions on 16 samples listed in Table II, none was rejected due to anomalous resistance or unstable J/V response. The mean resistances observed for PPF/NAB(3.7)/Cu/Au junctions are shown in Fig. 4 for two residual gas pressures, and exhibit only a weak dependence on pressure. Comparison of Tables I and II reveals that the Cu junctions consistently had lower resistance than the corresponding low oxide Ti junctions, often by about 50%.

An additional difference between the Ti and Cu junctions was stability during exposure to air. The resistance of the low oxide Ti junctions increased with time, by roughly a factor of 100 over a period of one month. J/V curves for 1-year-old Ti junctions showed rectification and hysteresis similar to that of the high oxide case of Fig. 1, but with smaller currents. The resistance also increased with time for PPF/NAB/Cu junctions, but much more slowly, by less than 10% per week in ambient air. As noted earlier, the resistance values reported here are from junctions measured one day after E-beam metal deposition, unless indicated otherwise. As the behavior of NAB/Ti junctions is likely to be affected by the semiconducting nature of TiO_x, identical junctions were fabricated with Al substituted for Ti. Not only is Al oxide an insulator, but it also lacks the intermediate oxidation states prevalent in the TiO_x deposit. A J/V curve for a 1-day-old PPF/NAB(3.7)/Al/Au junction prepared under high oxide conditions is included in Fig. 5a and c. The Al oxide junction had very high resistance, no rectification, and no hysteresis, for a voltage range of at least ±4 V.

Because the resistance values for Cu and low oxide Ti junctions are low, a concern arises that Cu penetrated the molecular layer and the observed response is due to Cu or Ti filaments or "shorts" acting as metallic conductors. This possibility was explored by making NAB and NBP junctions with varying thickness by exploiting their propensity to form multilayers.[19] J/V curves for junctions consisting of three thicknesses of NAB with both Ti and Cu top contacts are shown in Fig. 6, and the observed resistances are listed in Tables I and II. The observed resistance increases rapidly with the thickness of the molecular layer for both Ti and Cu top contacts.

Inspection of Fig. 5 and 6 reveals that the i/V curves approach a similar slope at high bias. The value of dV/di at both positive (Tables I and II) and negative bias (not shown) is in the range of 150-300 Ω, slightly higher than the observed low bias resistance when the molecule is absent. These observations imply that the current at high bias is limited by the background resistance, which results mainly from the relatively high resistivity of PPF (0.005 Ω-cm).[16,17] Figure 7a shows the PPF/NAB/Cu/Au current/voltage curves corrected for a constant series resistance of 150 Ω, by subtracting the iR product from the applied voltage. Figure 7b shows a plot of differential conductance (di/dV) *vs.* V for a PPF/NAB(4.2)/Cu/Au junction, as well as the control plot for a junction with no molecular layer. The high conductance for the corrected curves at high bias implies rapid electron transport through the molecular layer.

Discussion

Considered as a group, the molecular junctions studied here can be classified into three distinct types, all of which are illustrated in

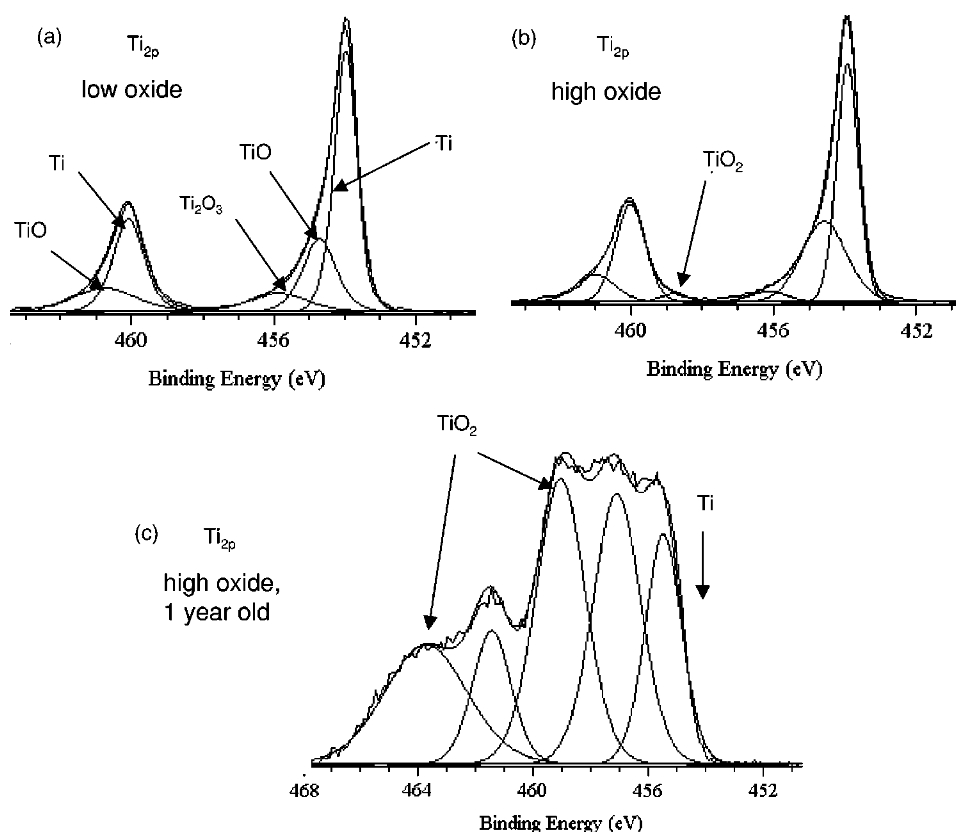

Figure 3. XPS spectra of PPF/azobenzene/Ti/Au junctions prepared with deposition pressure of (a) 8.0×10^{-6} Torr and (b) 2.1×10^{-7} Torr, following Ar^{+} sputtering of junction for 1500 s. Sputtering time was chosen to remove most of the Au and Ti overlayers, so the composition reflects that near the molecular layer. Spectrum (c) is high oxide junction after exposure to lab air for ~1 year. Likely assignments for various peaks are shown.

Fig. 1 and 5. The PPF/NAB(3.7)/Cu/Au junctions have limited oxide present and are essentially carbon/molecule/metal junctions with relatively high conductivity. The high oxide PPF/NAB(3.7)/Al/Au junctions have very low conductivity and appear to be carbon/molecule/insulator/metal junctions. The important distinctions between AlO_x and TiO_x include the semiconducting behavior of TiO_x and the existence of intermediate oxidation states between Ti(0) and Ti(IV), which are not present for AlO_x. Therefore, the high oxide PPF/NAB(3.7)/Ti/Au junctions appear to be carbon/molecule/semiconductor/metal devices with different behavior from that of the Cu and Al junctions. The following discussion considers the consequences of variations in the nature of the metal layer with deposition conditions and composition.

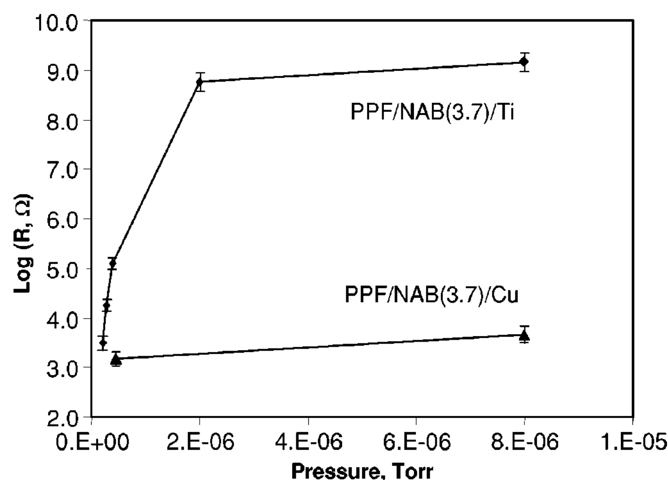

Figure 4. Mean resistances (on log scale) of PPF/NAB(3.7)/Ti/Au and PPF/NAB(3.7)/Cu/Au junctions prepared with a range of residual gas pressures during Ti or Cu deposition. Error bars represent ±1 standard deviation unit. In all cases, initial Ti or Cu deposition rate was 0.1 nm/s.

The dramatic effect of residual gases on PPF/molecule/Ti/Au junctions apparent in Fig. 1-3 indicates the importance of Ti oxides to junction behavior, a point that was not appreciated when such junctions were described initially.[13,15] Let us first discuss the low oxide Ti junctions and Cu junctions listed in Table I, because they represent the conceptually simplest case. Figure 3 shows that substantial Ti oxide is present for the lowest backpressure studied, and the continuing decrease in resistance with pressure (Fig. 4) implies that the resistance for a junction of purely metallic Ti is lower than that observed for Ti deposition at 2.1×10^{-7} Torr. The redox potential of Cu ($E° = 0.34$ *vs.* normal hydrogen electrode) is nearly 2 V positive of Ti (−1.6 V), and the sticking coefficient of oxygen on Cu is at least four orders of magnitude lower than that on Ti.[31] Hence, Cu should be much less prone to react with residual H_2O or O_2 during E-beam deposition. As shown in Fig. 4, the resistance observed for PPF/NAB(3.7)/Cu junctions is much less sensitive to residual gases and has a resistance near that of the lowest oxide Ti junction. Based on the initial results with copper as a top contact, it appears that it is yielding junctions with characteristics similar to those made using titanium, but with much lower likelihood of insulating oxide formation.

A strong indication that junction behavior reflects the properties of the molecule rather than some artifact is the pronounced effect of molecular structure and film thickness on conductivity, shown in Fig. 1, 2, and 6. Even if the i/V response were contaminated by defects or metallic short circuits, the large variation in conductivity and curve shape for different molecules indicates that the molecule is a major factor in determining junction conductivity. For example, the high oxide NAB response of Fig. 1 is qualitatively different from that of the high oxide BP junction (Fig. 2), lacking the hysteresis at negative voltage. Furthermore, Table I shows variations of a factor of 35 for molecules of nearly the same length (BP and NBP) and a

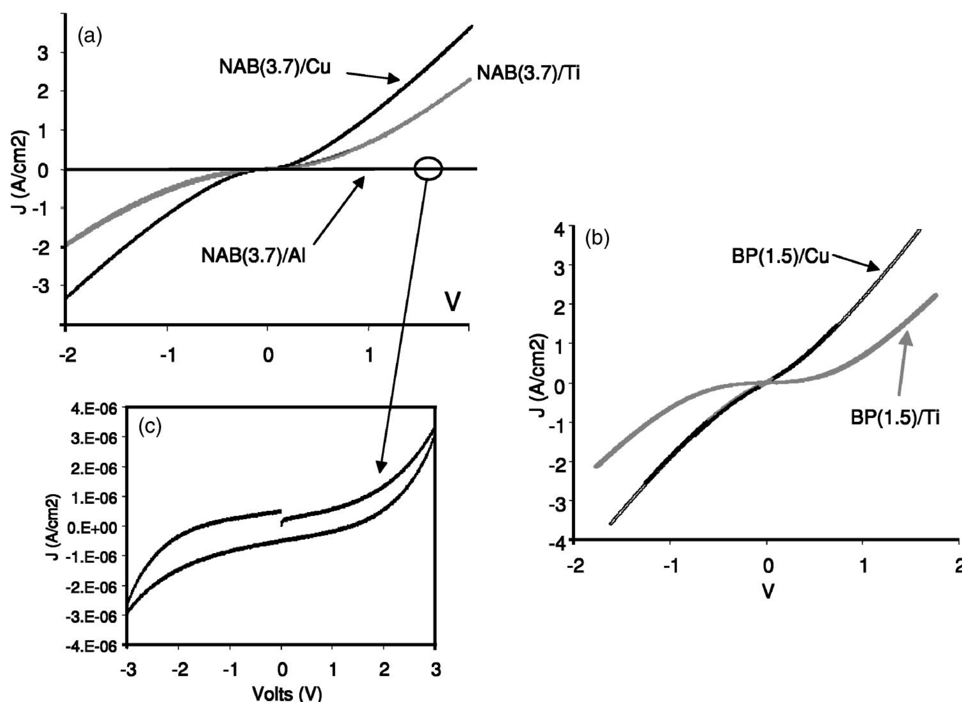

Figure 5. Comparison of J/V (1000 V/s) curves for (a) NAB and (b) BP junctions prepared with Cu top contacts deposited at 4.5×10^{-7} Torr (NAB) or 2.7×10^{-7} Torr (BP) or Ti top contacts deposited at 2.1×10^{-7} Torr. Panel a also includes J/V curve with aluminum substituted for Ti using high oxide conditions; this curve is magnified in panel c.

factor of over 200 for different molecular layer thicknesses [NBP(1.7) and NBP(4.2)]. These variations are difficult to explain unless the nature and thickness of the molecular layer are strong determinants of junction conductivity.

Given past reports of metal penetration into Au/thiol SAMs,[1-5] how do we know the i/V curves observed for Cu junctions are not merely due to metallic filaments? Although the observed resistances for NAB, BP, and NBP monolayers with Cu contacts (443, 315, and 267 Ω, respectively) are close to each other, there are several strong arguments against the involvement of metallic Cu "short circuits." First, metallic conduction through Cu should be linear with voltage, rather than showing the nonlinear behavior apparent in Fig. 1, 2, and 5-7. The possibility that the nonlinear i/V response results from formation of Cu or Ti filaments at high bias is unlikely, given the repeatability and scan rate independence (from 0.1 to 1000 V/s) of the i/V curves. Second, metallic conduction should show a weak dependence on layer thickness ($\sim d^{-1}$), yet both NBP and NAB show a much stronger dependence, with resistance increasing by factors of 20-200 for a factor of $\sim$3 increase in the thickness of the molecular layer. Third, the good reproducibility of the resistance of Cu junctions is unlikely if the conductivity is controlled by metallic defects, unless the defects are numerous and uniform. Furthermore, the "blank" junctions without molecules exhibit linear i/V curves, with a slope reproducibly higher than that observed for molecular junctions (Fig. 1, Tables I and II, bottom entry). Fourth, the similarity of junction resistance for BP, NBP, and NAB monolayers is at least partly due to the background resistance of 80-250 Ω. Subtraction of this resistance amplifies the structural effects, implying a stronger dependence of conductivity on molecular structure. This correction is not yet rigorous enough to draw quantitative conclusions about the structural effects on monolayer junction resistance, but such differences are unlikely if conductivity were due solely to metallic "shorts." Finally, if recently reported resistances for similar molecules (*e.g.*, 4,4′-bipyridine, 1.3 MΩ)[32] are scaled up to junctions with $\sim 10^{11}$ molecules in parallel, the observed junction resistances should be less than 1 Ω without invoking metal filaments. This observation does not prove that filaments are absent, but it does indicate that low observed resistances for the current monolayer junctions are consistent with reported single molecule results. Although pinholes or other defects cannot be totally ruled out for the Cu junctions, the strong dependence of junction behavior on the structure and thickness of the molecular layer indicates that such defects cannot be the dominant determinant of junction conductivity. It is likely that the ability to make functioning reproducible molecular junctions by metal deposition on the monolayers studied here is due to the strength of the substrate-molecule bond ($\sim$100 kcal/mol) compared to much weaker Au-thiol ($\sim$40 kcal/mol) bonds in SAMs and electrostatic bonds in LB structures.

The symmetry of the low oxide Ti and Cu junctions implies that the work function difference between the metal and carbon does not induce significant rectification. The strong rectification reported previously[13,33] for high oxide Ti junctions requires TiO_x to be present and is completely absent for the Cu junctions. The observation that the Cu and low oxide Ti junctions all exhibit high conductivity for high bias could be due to several mechanisms, including resonant tunneling through unoccupied molecular orbitals, thermionic (*i.e.*, Schottky) or field (*i.e.*, Fowler-Nordheim) emission. Detailed studies of temperature dependence and curve shape are currently underway to probe the conductivity mechanism.

The XPS results in Fig. 3 indicate a mixture of Ti(0), Ti(II), Ti(III), and Ti(IV), all in a presumably disordered oxide deposit. The absence of hysteresis for the low oxide Ti junctions implies a change in mechanism associated with the presence and composition of the TiO_x layer. The small difference in the XPS results for high and low oxide junctions is surprising, given the large change in electronic properties. A possible explanation is based on the observation that the TiO_2 content increases with time, presumably by permeation of oxygen or water through the protective Au film covering the Ti layer. TiO and Ti_2O_3 are only slightly less conductive than Ti metal,[34] but TiO_2 has a conductivity approximately 10 orders of magnitude lower. Thus, small amounts of TiO_2, possibly formed as a layer at the Au/Ti interface, could have large effects on conductivity. This possibility is supported by the observation that "old" junctions with signficantly higher TiO_2 content (Fig. 3c) have very low conductivity and exhibit pronounced hysteresis. Although the junction composition and structure were very different from the current case, Hoagland *et al.*[35] reported that Cu/molecule/Al tunnel junctions were also sensitive to residual gases, and they attributed

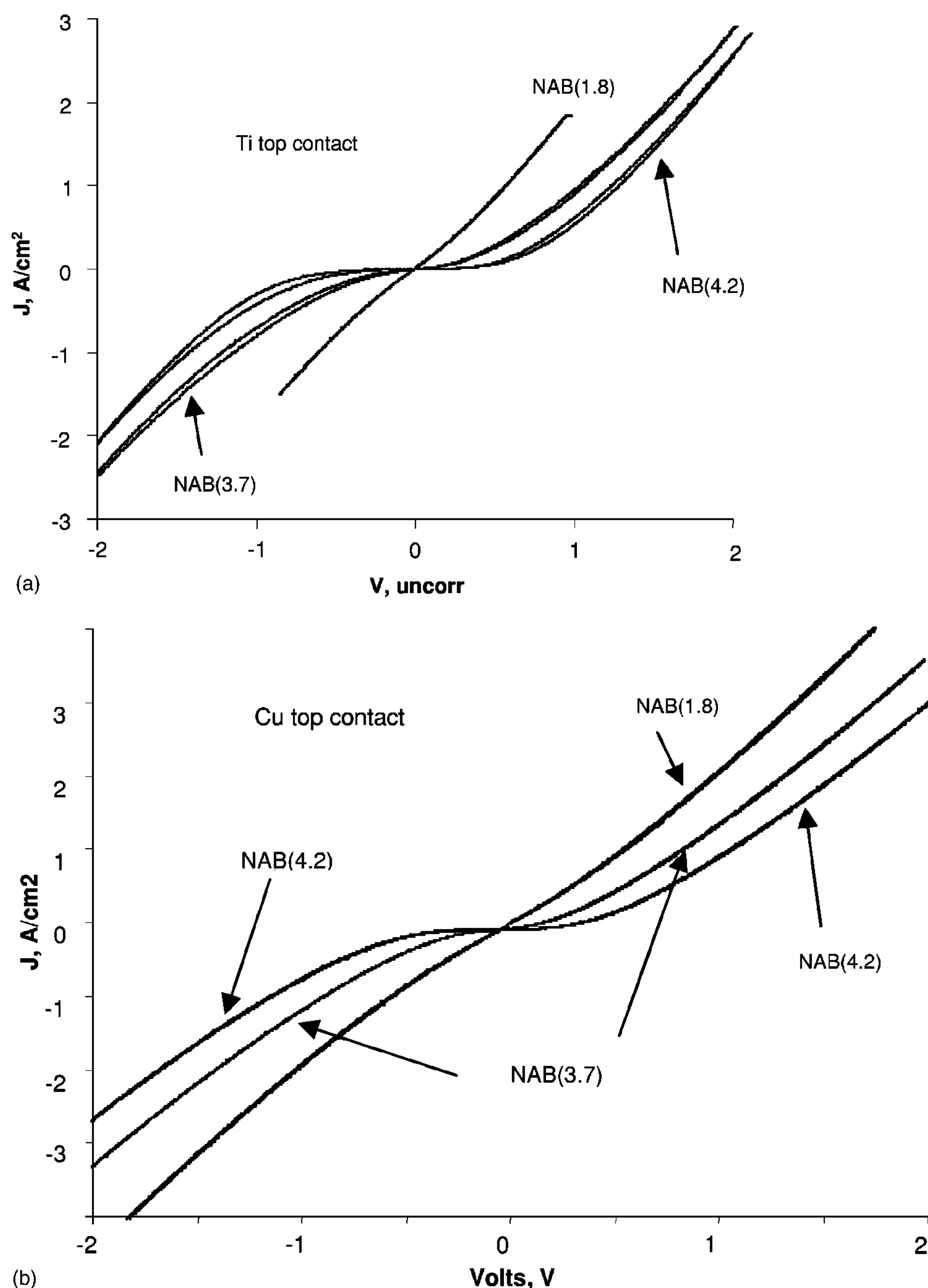

Figure 6. J/V curves for junctions of varying NAB thickness, both (a) Ti and (b) Cu top contacts. Ti deposited at 2.1×10^{-7} Torr, Cu at 4.5×10^{-7} Torr.

the effect to aluminum oxide formation. As apparent in Fig. 5a, a carbon/NAB/metal junction has high conductivity, and addition of an AlO_x insulating oxide results in very low conductivity. The semiconducting Ti oxide junction not only has an intermediate conductivity, but it also exhibits hysteresis and rectification.

Electron transfer in carbon/molecule/Ti high oxide junctions is under active investigation, but at least two mechanisms may be responsible for the increase in current and hysteresis under positive bias. We showed previously using Raman spectroscopy that NAB on PPF is partially reduced upon Ti deposition to a mixture of NAB and NAB anion radical.[14] In a separate publication, we reported structural changes in high oxide PPF/NAB/Ti/Au junctions observed *in situ* with Raman spectroscopy through a partially transparent metal top contact.[33] The spectra showed unequivocally that structural changes occurred in the NAB layer under negative bias (PPF relative to Ti), and that these changes were similar to those observed during electrochemical reduction of NAB chemisorbed to glassy carbon.[36] It was also apparent during the spectroscopic experiment that both NAB and TiO_x must be present for rectification to be observed.[33] Therefore, the conductance changes and hysteresis observed in high oxide PPF/NAB/Ti junctions are associated with a redox process in which electrons are transferred between the NAB/NAB^- and Ti/TiO_x layers. An applied voltage in the range of 2-3 V should be energetically sufficient to cause redox reactions, given that the difference in redox potentials between NAB in acetonitrile (-0.62 V *vs.* NHE[36]) and Ti/Ti^{+2} (-1.6 V) is about 1 V. Solution redox potentials are only a guide to solid-state behavior, but clearly, a negative bias on a PPF/NAB/Ti junction promotes formation of NAB anion at the negative electrode, whereas a positive bias should oxidize NAB anion and inject electrons into the Ti/TiO_x layer. One explanation for the hysteresis in high oxide junctions is a change in Ti/TiO_x or NAB/NAB^- conductivity accompanying such electron injection. This injection may provide charge carriers in the semicon-

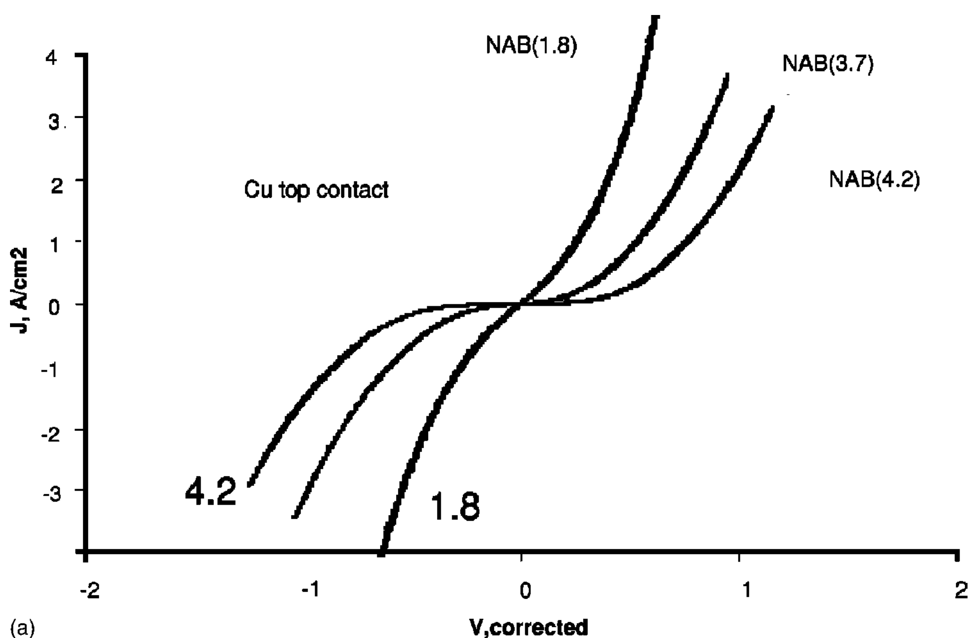

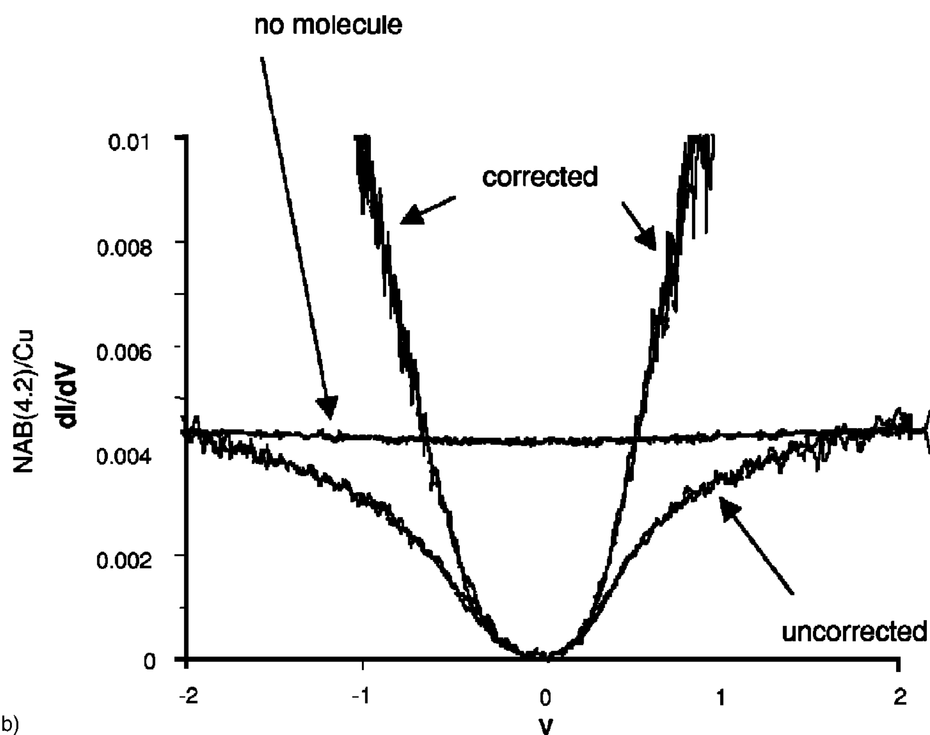

Figure 7. (a) J/V curves for PPF/NAB/Cu/Au junctions (from Fig. 6b) after correction of the voltage axis for background resistance. The product iR was subtracted from the applied voltage before plotting, with $R = 150\ \Omega$. (b) Differential conductance (di/dV) for PPF/NAB(4.2)/Cu/Au curve for Fig. 6b, uncorrected and corrected for 150 Ω of ohmic potential error. Also shown is an uncorrected curve for a "blank" PPF/Cu/Au junction with molecule absent.

ducting TiO_x or may produce Ti metal, which provides metallic conductivity between the bulk Ti metal and the molecular layer. It is also possible that the insulating TiO_2 present in high oxide Ti junctions is reduced to the more conductive Ti(II) or Ti(III) oxides. In any case, electron injection into the initial, low conductivity TiO_x generates a more conductive phase under positive bias, while electrons leave the molecular layer. In the limit of complete conversion of TiO_x to a metallic phase, we expect the junction conductivity to approach that of the low oxide case, as is apparent in Fig. 1 and 5. As reported in detail previously,[13] this electron injection process has several properties of a redox reaction, including dependence on temperature, time, and applied voltage. The hysteresis results from the relatively slow kinetics of the overall reaction. Note that biphenyl and nitrobiphenyl are also reducible to anion radicals, although at more negative potentials than NAB. The stoichiometry of the redox process depends on the products of the reactions of trace gases with deposited titanium, and it is difficult to narrow down the possible reactions without more information about TiO_x composition. Furthermore, observed conductivity is a function of the electronic properties of both the TiO_x and NAB layers, both of which are modified by a redox process. Nevertheless, the key point is the association between electron transfer between the NAB and TiO_x phases and changes in junction conductivity.

Conclusion

In summary, the behavior of carbon/molecule/metal molecular junctions is a strong function of preparation conditions, particularly those that result in a semiconducting metal oxide layer. Reduction of residual gas pressure during metal deposition causes the junction current/voltage behavior to change from the rectification reported

previously[13,15] to a symmetric response with much higher current density. The extreme sensitivity of titanium to trace gases is a likely source of the greater variability in Ti junction resistance and behavior compared to Cu. If the residual gases were controlled more accurately than possible with the apparatus used here, this variability should be reduced. Cu junctions are distinct from Ti junctions and more closely resemble a true carbon/molecule/metal structure. For Ti or other metals, control of oxide level may permit useful exploitation of the hysteresis and rectification associated with the oxide, *e.g.*, in memory devices based on the conductivity of various redox states. It is somewhat speculative at this point, but it is also possible that trace water or oxygen is actually beneficial during Ti deposition, in that it allows TiO_x formation in lieu of "destruction" of the monolayer by titanium atoms reported for SAMs.[11,12] However, for fundamental investigations of electron transport in molecules, copper appears to be superior to titanium, with its much lower sensitivity to residual gases. The next step using a Cu top contact is to significantly reduce the junction area to minimize effects of ohmic potential losses in the PPF and external contacts, and to exclude air from completed junctions to improve junction stability.

Acknowledgments

This work was supported by the National Science Foundation through project 0211693 from the Analytical and Surface Chemistry Division, and by ZettaCore, Inc..

The Ohio State University assisted in meeting the publication costs of this article.

References

1. G. L. Fisher, A. E. Hooper, R. L. Opila, D. R. Jung, D. L. Allara, and N. Winograd, *J. Phys. Chem. B*, **104**, 3267 (2000).
2. G. L. Fisher, A. Hooper, R. L. Opila, D. R. Jung, D. L. Allara, and N. Winograd, *J. Electron Spectrosc. Relat. Phenom.*, **98-99**, 139 (1999).
3. G. L. Fisher, A. V. Walker, A. E. Hooper, T. B. Tighe, K. B. Bahnck, H. T. Skriba, M. D. Reinard, B. C. Haynie, R. L. Opila, N. Winograd, and D. L. Allara, *J. Am. Chem. Soc.*, **124**, 5528 (2002).
4. A. Hooper, G. L. Fisher, K. Konstadinidis, D. Jung, H. Nguyen, R. Opila, R. W. Collins, N. Winograd, and D. L. Allara, *J. Am. Chem. Soc.*, **121**, 8052 (1999).
5. K. Konstadinidis, P. Zhang, R. L. Opila, and D. L. Allara, *Surf. Sci.*, **338**, 300 (1995).
6. C. Zhou, M. R. Deshpande, M. A. Reed, L. Jones, and J. M. Tour, *Appl. Phys. Lett.*, **71**, 611 (1997).
7. S.-C. Chang, Z. Li, C. N. Lau, B. Larade, and R. S. Williams, *Appl. Phys. Lett.*, **83**, 3198 (2003).
8. D. R. Stewart, D. A. A. Ohlberg, P. A. Beck, Y. Chen, R. S. Williams, J. O. Jeppesen, K. A. Nielsen, and J. F. Stoddart, *Nano Lett.*, **4**, 133 (2004).
9. Y. Chen, D. A. A. Ohlberg, X. Li, D. R. Stewart, R. S. Williams, J. O. Jeppesen, K. A. Nielsen, J. F. Stoddart, D. L. Olynick, and E. Anderson, *Appl. Phys. Lett.*, **82**, 1610 (2003).
10. Y. Chen, G.-Y. Jung, D. A. A. Ohlberg, X. Li, D. R. Stewart, J. O. Jeppesen, K. A. Nielsen, J. F. Stoddart, and R. S. Williams, *Nanotechnology*, **14**, 462 (2003).
11. B. C. Haynie, A. V. Walker, T. B. Tighe, D. L. Allara, and N. Winograd, *Appl. Surf. Sci.*, **203-204**, 433 (2003).
12. B. d. Boer, M. M. Frank, Y. J. Chabal, W. Jiang, E. Garfunkel, and Z. Bao, *Langmuir*, **20**, 1539 (2004).
13. R. L. McCreery, J. Dieringer, A. O. Solak, B. Snyder, A. Nowak, W. R. McGovern, and S. DuVall, *J. Am. Chem. Soc.*, **125**, 10748 (2003).
14. A. M. Nowak and R. L. McCreery, *Anal. Chem.*, **76**, 1089 (2004).
15. R. McCreery, J. Dieringer, A. O. Solak, B. Snyder, A. M. Nowak, W. R. McGovern, and S. DuVall, *J. Am. Chem. Soc.*, **126**, 6200 (2004).
16. S. Ranganathan, R. L. McCreery, S. M. Majji, and M. Madou, *J. Electrochem. Soc.*, **147**, 277 (2000).
17. S. Ranganathan and R. L. McCreery, *Anal. Chem.*, **73**, 893 (2001).
18. J. H. Moore, C. C. Davis, and M. A. Coplan, *Building Scientific Apparatus: A Practical Guide to Design and Construction*, Allan M. Wylde, 1989.
19. F. Anariba, S. H. DuVall, and R. L. McCreery, *Anal. Chem.*, **75**, 3837 (2003).
20. D. Simon, C. Perrin, and J. Bardolle, *J. Microsc. Spectrosc. Electron.*, **1**, 175 (1976).
21. A. R. Gonzalez-Elipe, G. Munvera, J. P. Espinos, and J. M. Sanz, *Surf. Sci.*, **220**, 368 (1989).
22. F. Werfel and O. Brummer, *Phys. Scr.*, **28**, 92 (1983).
23. J. F. Moulder, W. F. Stickle, W. F. Sobol, and K. D. Bomben, *Handbook of X-Ray Photoelectron Spectroscopy*, Perkin-Elmer Corp., Eden Prairie, MN (1992).
24. R. P. Netterfield, P. J. Martin, C. G. Pacey, W. G. Sainty, and D. R. McKenzie, *J. Appl. Phys.*, **66**, 1805 (1989).
25. D. Gonbeau, C. Guimon, G. Pfister-Guillouzo, A. Levasseur, G. Meunier, and R. Dormoy, *Surf. Sci.*, **254**, 81 (1991).
26. C. D. Wagner, D. A. Zatko, and R. H. Raymond, *Anal. Chem.*, **52**, 1445 (1980).
27. T. Dickinson, A. F. Povey, and P. M. A. Sherwood, *J. Chem. Soc., Faraday Trans. 1*, **72**, 686 (1976).
28. C. D. Wagner, D. E. Passoja, H. F. Hillery, T. G. Kinisky, H. A. Six, W. T. Jansen, and J. A. Taylor, *J. Vac. Sci. Technol.*, **21**, 933 (1982).
29. J. Haber, J. Stoch, and L. Ungier, *J. Electron Spectrosc. Relat. Phenom.*, **9**, 459 (1976).
30. N. S. McIntyre, S. Sunder, D. W. Shoesmith, and F. W. Stanchell, *J. Vac. Sci. Technol.*, **18**, 714 (1981).
31. E. Fromm and O. Mayer, *Surf. Sci.*, **74**, 259 (1978).
32. B. Xu and N. J. Tao, *Science*, **301**, 1221 (2003).
33. A. M. Nowak and R. L. McCreery, *J. Am. Chem. Soc.*, **126**, 16621 (2004).
34. D. Mardare, C. Baban, R. Gavrile, M. Modreanu, and G. I. Rusu, *Surf. Sci.*, **507-510**, 468 (2002).
35. J. J. Hoagland, X. D. Wang, and K. W. Hipps, *Chem. Mater.*, **5**, 54 (1993).
36. T. Itoh and R. L. McCreery, *J. Am. Chem. Soc.*, **124**, 10894 (2002).